Food Hydrocolloids 51 (2015) 41–53

Contents lists available at ScienceDirect

Food Hydrocolloids

journal homepage: www.elsevier.com/locate/foodhyd

Acacia senegal vs. Acacia seyal gums – Part 1: Composition and structure of hyperbranched plant exudates

Lizeth Lopez-Torrez [a, b, *], Michaël Nigen [a], Pascale Williams [c], Thierry Doco [c], Christian Sanchez [a]

[a] UMR 1208 Ingénierie des Agropolymères et Technologies Emergentes, Montpellier SupAgro-INRA-Université de Montpellier2-CIRAD, 2 Place Pierre Viala, 34060, Montpellier Cedex 1, France
[b] Alland & Robert, 9 rue Saintonge, 75003, Paris, France
[c] UMR 1083 Sciences Pour l'Œnologie, Montpellier SupAgro, INRA, Université de Montpellier2, 2 Place Pierre Viala, 34060, Montpellier Cedex 1, France

ARTICLE INFO

Article history:
Received 3 November 2014
Received in revised form
28 February 2015
Accepted 5 April 2015
Available online 30 April 2015

Keywords:
Acacia gum
Arabinogalactan-protein
Hyperbranched structure
HPSEC MALLS
Ellipsoid conformation

ABSTRACT

Acacia gum is a natural arabinogalactan-protein type polysaccharide widely used in industrial applications. The two varieties of Acacia gum, *A. senegal* and *A. seyal*, are hyperbranched polysaccharides rich in arabinose and galactose (PRAG) mainly formed by chains of 3,6-linked β-D-Gal*p* substituted in position 6 by side chains of 3-linked α-L-Ara*f*. Beyond this common structure, *A. senegal* presented the highest degree of branching (78.2% vs. 59.2%) with more branched galactopyranoses, shorter arabinosyl side branches, and more rhamnopyranoses in terminal position. Circular dichroism experiments evidenced that both Acacia gums were partially structured into polyproline type II helices but in a lesser extent for *A. senegal* gum, suggesting its less structured organisation. The fingerprint of both Acacia gums and their spectral differences determined by FTIR spectroscopy were described. Analysis of HPSEC-MALLS data suggested that macromolecules of both Acacia gums adopted an ellipsoid-like conformation in solution. The average molecular weight of *A. seyal* macromolecules was larger than that of *A. senegal* ones (8.2×10^5 g mol^{-1} vs. 6.8×10^5 g mol^{-1}). Nevertheless, *A. seyal* macromolecules appeared more compact and less viscous (R_g: 17.1 nm; [η]: 16.5 mL g^{-1}) than *A. senegal* ones (R_g: 30.8 nm; [η]: 22.8 mL g^{-1}). The most compact structure of *A. seyal* gum can be partly explained by the lowest concentration of charged sugars that induces less electrostatic repulsion, and the highest content of long arabinose side chains that may self-organize and interact between them (e.g. hydrogen bonding, steric effect, etc.). For both Acacia gums, the anisotropy of macromolecules increased with the molecular weight, however, *A. senegal* macromolecules were the most anisotropic ones.

1. Introduction

Acacia gum, also called gum Arabic, is an edible ingredient (AG, E 414 EC) largely used as emulsifier, stabiliser, and coating agent in food and non-food applications. Acacia gum is defined as the air-dried exudation from branches and stem of *Acacia senegal* (L) Willdenow trees or closely related species such as *Acacia seyal* (family Leguminosae) (FAO., 1999). It is found in nature as polysaccharidic acid rich in calcium, magnesium, and potassium salts (Islam, Phillips, Sljivo, Snowden, & Williams, 1997; Kennedy, Phillips, & Williams, 2010; Verbeken, Dierckx, & Dewettinck, 2003). Acacia gum typically contains highly branched complex arabinogalactan-proteins (AGP), ubiquitary biopolymers in plant kingdom implicated in several development and growth functions, such as differentiation, cell–cell recognition, embryogenesis, programmed cell death, and also in plant–pathogen interactions (Ellis, Egelund, Schultz, & Bacic, 2010; Gaspar, Johnson, McKenna, Bacic, & Schultz, 2001). Acacia gum is mainly composed by D-galactose, L-arabinose, L-rhamnose, D-glucuronic acid, and *4-O-methyl*-D-glucuronic acid with a small fraction of proteins. Its biochemical composition and molecular characteristics can vary depending on internal and external factors (Acacia specie, tree location, age of

* Corresponding author. UMR 1208 Ingénierie des Agropolymères et Technologies Emergentes, Montpellier SupAgro-INRA-Université de Montpellier2-CIRAD, 2 Place Pierre Viala, 34060, Montpellier Cedex 1, France. Tel.: +33 4 99 61 28 90; fax: +33 4 99 61 30 76.
E-mail addresses: lizeth.lopez@supagro.inra.fr (L. Lopez-Torrez), michael.nigen@supagro.inra.fr (M. Nigen), pascale.williams@supagro.inra.fr (P. Williams), thierry.doco@supagro.inra.fr (T. Doco), sanchez@supagro.inra.fr (C. Sanchez).

http://dx.doi.org/10.1016/j.foodhyd.2015.04.019
0268-005X/

trees, weather conditions, and site and way of tapping) and post-harvesting processes (storage conditions, maturation time, filtration, high pressure homogenisation, spray drying, irradiation, or heat treatments) (Al-Assaf, Andres-Brull, Cirre, & Phillips, 2012; Al-Assaf, Sakata, McKenna, Aoki, & Phillips, 2009; Anderson, Bridgeman, & De Pinto, 1984; Anderson & Farquhar, 1979; Chikamai, Banks, Anderson, & Weiping, 1996; Idris, Williams, & Phillips, 1998; Phillips, 2009).

Basically, the highly branched polysaccharidic structure consists of 1,3-linked β-D-galactopyranose monomers with side branches linked to the main chain mainly through substitution at O-6 position. Units of α-L-arabinofuranosyl and α-L-rhamnopyranosyl are distributed in the main and side chains while β-D-glucuronopyranosyl and 4-*O*-*Methyl*-β-D-glucuronopyranosyl are mostly end-units (Anderson, Hirst, & Stoddart, 1966; Anderson & Stoddart, 1966). Street and Anderson (1983) proposed that Acacia gum structure could be explain in terms of repeated fragments. The former, *Acacia senegal*, would be composed mainly by repeated fragments of ramified chains of galactose with arabinose side chains of varying length and glucuronic and 4-*O*-*Me*-glucuronic acids end units (Type I). In contrast, the structure of *Acacia seyal* would be a mix of two or three ramified fragments type I with significant single units of galactose linked to one arabinose chain of varying length (Type II) (Street & Anderson, 1983). The structure of *A. senegal* was suggested to be more ramified and more regular than the *A. seyal* structure. Recently, Nie et al. (2013a, 2013b) proposed structural models for the polysaccharide backbone of *A. senegal* and *A. seyal* gums based on the previous work of Street and Anderson (1983), with substitution of side chains at O-6, O-2, or O-4 positions. Polysaccharide chains are linked to proteins by covalent links in serine- and hydroxyproline-rich domains (Akiyama, Eda, & Kato, 1984; Anderson & McDougall, 1987; Qi, Fong, & Lamport, 1991). Typically, *A. senegal* gum is richer in protein than *A. seyal* (1.8% wt vs. 0.9% wt respectively) (Islam et al., 1997).

Acacia gums were always described as heterogeneous, polydisperse, and hetero-polymolecular system having more than one component with different monomer composition, molecular weight, and mode of linking and branching (Anderson & Stoddart, 1966; Islam et al., 1997; Renard, Lavenant-Gourgeon, Ralet, & Sanchez, 2006). Using hydrophobic interaction chromatography (HIC) or size exclusion chromatography (SEC), multiple macromolecular fractions were separated from *A. senegal* gum (Anderson et al., 1984; Randall, Phillips, & Williams, 1989; Renard et al., 2006; Vandevelde & Fenyo, 1985). The three main fractions obtained by HIC were named the arabinogalactan (AG) fraction, the arabinogalactan-protein (AGP) fraction, and the glycoprotein (GP) fraction. The most abundant fraction, AG, represents approximately 85–90 % of the total gum with a molecular weight around 2.8×10^5 g mol^{-1} and traces of protein, a peptide of about 40 amino acids (Mahendran, Williams, Phillips, Al-Assaf, & Baldwin, 2008; Randall et al., 1989; Renard et al., 2006). The second main fraction, AGP, represents around 10% of total gum and contains ~12% of protein. The AGP fraction is generally composed of high molecular weight (M_w) macromolecules ($1 \times 10^6 < M_w < 4 \times 10^6$ g mol^{-1}) (Randall et al., 1989; Renard, Garnier, Lapp, Schmitt, & Sanchez, 2012). The minor GP fraction, around 2% of the total gum, contains the highest content of proteins around 25–40 %. This fraction is composed of at least three glycoprotein populations with molecular weight ranging from 2.5×10^5 to 2.6×10^6 g mol^{-1}. *A. seyal* gum was also fractionated using HIC and the three main molecular fractions obtained were also named AG, AGP, and GP (Siddig, Osman, Al-Assaf, Phillips, & Williams, 2005).

Acacia gum is one of the oldest gums used in industrial applications. In the past, most of scientific studies focused on the structural and physicochemical properties of *A. senegal* gum, while only few of them concerned the *A. seyal* gum. This can be explained by the main use of *A. senegal* gum in industrial applications and the relatively recent authorization of *A. seyal* gum in food and pharmaceutical industries (FAO., 1999). Therefore, since *A. seyal* gum has recently been gaining interest and relevance in the Acacia gum market, we carried out a complete comparative study for *A. senegal* and *A. seyal* gums for a better understanding of their functional properties. This first paper describes the biochemical and structural characterization of both Acacia gum varieties. The characterization of Acacia gums dealt with the biochemical analysis (neutral and acid sugars, protein, and amino acid composition) and the identification of glycosidic linkages involved in the polysaccharidic structure. Far UV circular dichroism, Fourier transform infrared spectroscopy, and size exclusion chromatography coupled on line to multi-detection (multi-angle laser light scattering, differential refractometer, UV, and differential viscosimeter) were also applied for elucidation of the structural properties of Acacia gums.

2. Materials and methods

2.1. Materials

Instant and soluble *Acacia senegal* (Lot N° OF110676) and *Acacia seyal* (Lot N° OF110724) gums were provided by ALLAND & ROBERT Company – Natural and organic gums (Port Mort, France). Raw nodules of *A. senegal* and *A. seyal* gums were collected in Sudan in 2011. Both Acacia gums followed the same purification process: elimination of insoluble materials by physical methods, pasteurisation, and spray drying. All other reagents were of analytical grade from Sigma-Aldrich (USA).

2.2. Demineralisation of Acacia gums

A. senegal and A. *seyal* gum powders were dissolved at 10 %w/w in ultra pure deionised water (18.2 mΩ resistivity) and left overnight at room temperature (20–25 °C) under gentle stirring for solubilisation. Solutions were centrifuged at 24500 *g* for 30 min at 20 °C and then extensively dialysed using a dialysis membrane (MWCO 12–14 kDa Spectra/Por® 2D) against deionised water for 48 h at room temperature. After dialysis, samples were centrifuged at 24500 *g* for 30 min at 20 °C and then freeze-dried.

2.3. Preparation of Acacia gum solutions

Freeze-dried Acacia gum was dissolved in ultra pure deionised water (18.2 mΩ resistivity) at the target concentration. Solutions were gently stirred for 24 h at room temperature (23–25 °C) and then centrifuged at 24500 *g* for 30 min at 20 °C for removing insoluble materials and air bubbles. The initial pH of solutions was comprised between 5.2 and 6.8 for both demineralised Acacia gums depending on their concentration (5–0.1 %w/w). The pH of samples was adjusted at 5 using HCl 1 N, HCl 0.1 N, or NaOH 0.5 N solutions to reproduce the natural pH of raw Acacia gum nodules in aqueous solution.

2.4. Chemical analyses

Moisture content and Ash content were determined according to the AOAC official method 925.10 and 923.03, respectively. Nitrogen content was determined using the Kjeldahl method and protein content was calculated using a conversion factor of 6.6. All chemical analyses were performed in duplicate.

2.5. Amino acid composition

Amino acids composition was determined after acid hydrolysis adding HCL 6 N to samples and heating samples at 110 °C for 24 h. The excess of acid was eliminated and hydrolysed samples were analysed by ionic exchange chromatography (BIOCHROM 30, Cambridge, UK) using lithium citrate 0.2 M at pH 2.2 as eluent. Analysis was done in triplicate and norleucine was used as internal standard.

2.6. Neutral sugars and uronic acids composition

Acacia gums are undergone to solvolysis with anhydrous MeOH containing 0.5 M HCl for 16 h at 80 °C, followed by per-O-trimethylsilylation of the methyl glycoside derivatives, in order to ascertain the neutral and acidic composition (Doco, O'Neill, & Pellerin, 2001). Freeze-dried samples of Acacia gum were dried at 45 °C for 4 h in presence of P_2O_5. Samples were mixed with 0.5 mL methanol chloride solution freshly prepared and were left at 80 °C for 16 h. The excess of hydrochloric acid was eliminated, and 0.33 mL of Tri-Sil® reagent (Pierce) was added to produce trisilylation of monosaccharides. Samples were left at 80 °C for 20 min, cooled down, and dried before addition of 0.5 mL of hexane to dissolve the TMS derivate. The clean hexane phase was analysed by gas chromatography (GC). The TMS derivatives were separated on two DB-1 capillary columns (30 m × 0.25 mm i.d., 0.25 μm film) (temperature programming 120–200 °C at 1.5 °C min^{-1}), coupled to a single injector inlet through a two-holed ferrule, with H_2 as the carrier gas on a Shimadzu GCMS-QP2010SE gas chromatograph. The outlet of one column was directly connected to a FID at 250 °C and the second column via a deactivated fused-silica column (0.25 m × 0.11 μm i.d.) was connected to a mass detector. Samples were injected in the pulsed split mode with a split ratio of 20:1. The transfer line to the mass was set at 280 °C. The mass spectra were obtained from *m/z* 50 to 400 every 0.2 s in the total ion-monitoring mode using an ion source temperature of 200 °C, a filament emission current of 60 μA, and an ionization voltage of 70 eV.

Neutral sugars were determined by the alditol acetates method. Briefly, neutral monosaccharides were released after hydrolysis of the isolated polysaccharide fraction with 2 M trifluoroacetic acid (75 min, 120 °C) (Albersheim, Nevins, English, & Karr, 1967). They were then converted to their corresponding alditiol acetates derivatives by reduction and acetylation; and they were quantified using GC analysis using a fused silica DB-225 capillary column (30 m × 0.32 mm i.d., 0.25 μm film; J&W Scientific) with hydrogen as carrier gas, on a Shimadzu GC-2010 *plus* gas chromatograph. The alditol acetates were identified from their retention times by comparison with standard monosaccharides. Experiments were done in triplicate and inositol was used as internal standard.

2.7. Polysaccharide structure analysis

Glycosyl linkage composition obtained by methylation analysis without prior carboxyl reduction of the uronic acid residues of the polysaccharide backbone structure was determined by gas chromatography coupled to electron ionization mass spectrometry (GC-EI-MS) of the partially methylated alditol acetates as previously described by Pellerin et al. (Pellerin et al., 1996). One miligram of Acacia gum in 0.5 mL of dimethyl sulfoxide was methylated using methyl sulfinyl carbanion and methyl iodide. The methylated materials were then treated with 2 M TFA for 1.15 h at 120 °C. The released methylated monosaccharides were converted to their corresponding alditols by treatment with $NaBH_4$ and then acetylated (Harris, Henry, Blakeney, & Stone, 1984). Partially methylated alditol acetates were analysed by GC-EI-MS on a Shimadzu GC-MS-QP2010SE gas chromatograph using two DB-1 capillary columns (30 m × 0.25 mm i.d., 0.25 μm film; temperature programming 135 °C for 3 min, then 1.2 °C min^{-1} to 180 °C) coupled to a single injector inlet through a two-holed ferrule. The outlet of one column was directly connected to a FID at 250 °C, and the second column was connected to a mass detector via a deactivated fused-silica column (0.25 m × 0.11 μm i.d.). Inositol was used as internal standard and to verify the rate of methylation. Response factors of partially methylated alditol acetates are those described by Sweet et al. (Sweets, Shapiro, & Albershein, 1975).The validity of the used methods and their repeatability were checked according to Vidal, Williams, Doco, Moutounet, and Pellerin (2003).

2.8. Far UV circular dichroism (UV-CD)

CD measurements in far UV region (190–260 nm) of Acacia gum solutions (2 %w/w; pH 5) were performed at 25 °C using a 0.1 cm cell path-length and a J-810 spectropolarimeter (Jasco, Japan). Spectra were recorded at 10 nm min^{-1} scan speed, with 1 nm bandwidth, and 4 s of integration time. Each spectrum was the average of four acquisitions corrected for the solvent contribution.

2.9. Fourier transform infrared spectroscopy (FTIR)

FTIR spectra of freeze-dried Acacia gum powders were acquired from 800 to 1900 cm^{-1} using an AVATAR 360 FTIR spectrometer (Nicolet, Missouri, USA). Each spectrum was the average of three acquisitions of 64 scans each recorded with a speed of 0.96 cm^{-1}. Scans were corrected for the air contribution and an automatic baseline was done for the region 800–1900 cm^{-1}. Spectra were analysed using OMNIC v7.1 software. For better identification of differences between Acacia gums, *A. senegal* spectrum was subtracted from *A. seyal* spectrum.

2.10. Multi-detector high performance size exclusion chromatography (HPSEC)

HPSEC experiments were performed using a Shimadzu HPLC system (Shimadzu, Japan) coupled to four detectors: multi-angle laser light scattering (MALLS) operating at eighteen angles (Dawn Heleos II, Wyatt, CA, USA), differential refractometer (Optilab T-rEX, Wyatt, CA, USA), on-line viscosimeter (VISCOSTAR II, Wyatt, CA, USA), and UV-VIS detector activated at 280 nm (SPD-20A, Shimadzu, Japan). The system was composed of one Shodex OHPAK SB-G pre-column followed by four columns in series (Shodex OHPAK SB 803 HQ, OHPAK SB 804 HQ, OHPAK SB 805 HQ and OHPAK SB 806 HQ).

Aqueous Acacia gum solutions (1 g L^{-1}; pH 5) were injected and eluted through the system with 0.1 M $LiNO_3$ solution containing 0.02% NaN_3 at a constant flow rate of 1 mL min^{-1} and 30 °C in triplicate. Data were analysed using ASTRA software 6.06 (Wyatt Technologies, Santa Barbara, CA). Average molecular weights (M_w), radius of gyration (R_g), intrinsic viscosity ([η]), and polydispersity index (M_w/M_n) were calculated using a refractive index increment (*dn/dc*) of 0.145 mL g^{-1} as previouosly identified for the most abundant population of Acacia gum (AG fraction) (Renard et al., 2006).

3. Results and discussion

3.1. Biochemical composition and polysaccharidic structure

The biochemical composition (water, protein, sugar, and ash content in dry basis) of Acacia gums is given in Table 1. *A. senegal* and *A. seyal* gums were composed mainly of sugars with similar

Table 1
Biochemical composition of *A. senegal* and *A. seyal* gums in dry basis (mean ± standard deviation).

Component (mg g^{-1})	*A. senegal*	*A. seyal*
Total dry matter	889.0 ± 0.27	893,0 ± 0.02
Sugars[a]	940.0	950,0
Galactose (%)[b]	35.8 ± 1.20	36,9 ± 1.05
Arabinose (%)[b]	30.3 ± 2.50	47,6 ± 0.60
Rhamnose (%)[b]	15.5 ± 0.35	3,0 ± 0.30
Glucuronic acid (%)[b]	17.4 ± 1.15	6,7 ± 0.40
4-O-Me-Glucuronic acid (%)[b]	1.0 ± 0.05	5,8 ± 0.55
Proteins	27.0 ± 0.01	10,0 ± 0.04
Minerals	33.0 ± 0.24	40,0 ± 0.07

[a] Total content of sugars was calculated by the difference of proteins and minerals from 1000 mg g^{-1} in dry basis.
[b] Sugar composition was determined by GC-MS.

content of water and minerals. Both Acacia gums contained the same amino acids with a higher content of protein in *A. senegal* (2.7%) than in *A. seyal* (1.0%). Hyp, Ser, Leu, and Pro were the most abundant residues in that order (Table 2). They represented more than 55% of the total amino acids in each variety. Similar amino acid profiles were also identified in previous studies on Acacia gums from different origins (Idris et al., 1998; Menzies, Osman, Malik, & Baldwin, 1996). In addition, slight differences were observed in the relative distribution of some amino acids that were contained in lower proportions. *A. senegal* gum was the richest in Thr, His, and Lys with a relative difference of 26%, 19%, and 13%, while *A. seyal* was the richest in Ser, Asp, and Val with a relative difference of 17%, 11%, and 10%, respectively. Cys and Met were not detected in both samples.

Regarding the sugar content, both Acacia gums were rich in galactose and arabinose units like other gum exudates from Acacia *Gumiferae* and *Vulgares* species, including *A. senegal* and *A. seyal* (Anderson & Farquhar, 1979; Flindt, Al-Assaf, Phillips, & Williams, 2005; Menzies et al., 1996). Since these two sugar units were the main biochemical components of *A. senegal* and *A. seyal* gums, these gums can be viewed and named as Polysaccharide Rich in Arabinose and Galactose (PRAG) (Doco, Williams, & Cheynier, 2007). Both Acacia gums contained ~36% of galactose. The molar ratio of arabinose to galactose was 1.0 for *A. senegal* and 1.5 for *A. seyal*. This result was close to previous reported values, which ranged from 0.6 to 1.6 for *A. senegal* (Idris et al., 1998; Islam et al., 1997; Nie et al., 2013a; Renard et al., 2006), and around 1.3 for *A. seyal* (Anderson et al., 1984; Islam et al., 1997; Nie et al., 2013b).

Table 2
Amino acid composition for *A. senegal* and *A. seyal* gums in dry basis (mean ± standard deviation).

Amino acids (mg g^{-1})	Abrev.	*A. senegal*	*A. seyal*
Alanine	Ala	0.49 ± 0.04	0.22 ± 0.01
Arginine	Arg	0.31 ± 0.05	0.12 ± 0.00
Aspartic acid	Asp	1.24 ± 0.04	0.49 ± 0.04
Glutamic acid	Glu	0.92 ± 0.01	0.28 ± 0.003
Glycine	Gly	0.79 ± 0.004	0.25 ± 0.07
Histidine	His	1.37 ± 0.01	0.27 ± 0.01
Hydroxyproline	Hyp	6.26 ± 0.52	2.13 ± 0.19
Isoleucine	Ile	0.31 ± 0.02	0.13 ± 0.01
Leucine	Leu	1.83 ± 0.04	0.60 ± 0.03
Lysine	Lys	0.63 ± 0.02	0.12 ± 0.03
Phenylalanine	Phe	0.82 ± 0.05	0.21 ± 0.01
Proline	Pro	1.61 ± 0.14	0.56 ± 0.001
Serine	Ser	2.50 ± 0.05	0.95 ± 0.03
Threonine	Thr	1.42 ± 0.02	0.34 ± 0.02
Tyrosine	Tyr	0.31 ± 0.04	0.14 ± 0.02
Valine	Val	0.71 ± 0.0001	0.31 ± 0.07
Total amino acids		21.5 ± 0.47	7.1 ± 0.16

The Acacia gums showed some differences in the total content of arabinose, rhamnose, glucuronic acid, and *4-O-Me*-glucuronic acid units. The arabinose and *4-O-Me*-glucuronic acid units were more abundant in *A. seyal* than in *A. senegal*, while the rhamnose and the glucuronic acid units were more abundant in *A. senegal* than in *A. seyal*. Two types of uronic acids were identified in both Acacia gums by GC-MS: glucuronic acid and *4-O-Me*-glucuronic acid. Their contents were similar to those reported in literature (Anderson et al., 1966; Islam et al., 1997; Renard et al., 2006). However, recently, galacturonic acid was also found in *A. seyal* gum (Nie et al., 2013b). This result differed from previous studies and from our results, where no galacturonic acid was identified.

In addition to the sugar composition, important characteristic of the polysaccharidic structures were investigated by identification and quantification of the glycosidic linkages (Table 3). Methylations were repeated three times, and the yield of methylation was 75% and 65% for *A. senegal* and *A. seyal*, respectively. Similar methylations have been reported for arabinogalactan-type polysaccharides, such as purified PRAGS in wine (Anderson et al., 1966; Aspinall & Fairweather, 1965; Vidal et al., 2003).The ratio of terminal to branched residues was 0.8 and 0.5 for *A. senegal* and *A. seyal*, respectively, suggesting that *A. seyal* was methylated in a lower extent. One hypothesis for explaining this difference is the "plasticising" properties of arabinose-rich side chains which could protect the polysaccharidic backbone structure of *A. seyal* from a complete methylation. Likewise, arabinose-rich polysaccharides from resurrection plants play a crucial role to avoid plant desiccation and maintain cell wall flexibility by a re-organisation of the matrix (Moore, Farrant, & Driouich, 2008; Moore et al., 2013).

Results confirmed that the structures of both Acacia gums were mainly formed by a chain of β-D-Gal*p* linked at 1 → 3, as shown repeatedly in a number of studies (Anderson, 1966; Churms, Merrifield, & Stephen, 1983; Islam et al., 1997; Nie et al., 2013a, 2013b). The total content of Gal*p* with at least one 1 → 3 link was quite similar for both Acacia gums with 43.3% for *A. senegal* and 37.1% for *A. seyal*. In both gums, the most abundant glycosidic linkages were 1 → 3,6 Gal*p*, T-Ara*f*, and 1 → 3 Ara*f*, with few differences in their molar content between varieties. These three glycosidic linkages represented around 60% of all identified linkages for each gum. These results were comparable to values from other *A. senegal* studies (Goodrum, Patel, Leykam, & Kieliszewski, 2000; Islam et al., 1997). However, Nie et al. (2013a) reported also

Table 3
Mode of linkage of neutral monosaccharides from *A. senegal* and *A. seyal* gums determined by methylation analysis and expressed as the total molar fraction (mean ± standard deviation).

Glycosyl residue	Mode of linkage	*A. senegal*	*A. seyal*
2,3,4,6-Galactose[a]	T-Gal*p*	4.3 ± 0.05	tr
2,4,6-Galactose	1 → 3 Gal*p*	2.2 ± 0.20	2.4 ± 0.72
2,3,4-Galactose	1 → 6 Gal*p*	2.4 ± 0.08	2.6 ± 0.34
2,3,6-Galactose	1 → 4 Gal*p*	–	7.9 ± 0.72
2,6-Galactose	1 → 3.4 Gal*p*	2.8 ± 0.19	1.5 ± 0.04
2,4-Galactose	1 → 3.6 Gal*p*	23.8 ± 1.82	32.0 ± 0.64
2-Galactose	1 → 3.4.6 Gal*p*	14.5 ± 1.06	1.2 ± 0.10
2,3,5-Arabinose	T-Ara*f*	17.0 ± 2.30	12.5 ± 1.71
2,3,4-Arabinose	T-Ara*p*	1.6 ± 0.02	1.8 ± 0.09
3,4-Arabinose	1 → 2 Ara*p*	–	11.6 ± 0.04
3,5-Arabinose	1 → 2 Ara*f*	tr	6.0 ± 0.42
2,5-Arabinose	1 → 3 Ara*f*	16.4 ± 0.75	16.1 ± 0.30
2,3-Arabinose	1 → 5 Ara*f*	0.9 ± 0.04	1.3 ± 0.11
3-Arabinose	1 → 2.5 Ara*f*	–	tr
2,3,4-Rhamnose	T-Rha*p*	12.0 ± 0.03	2.3 ± 0.04
3,4-Rhamnose	1 → 2 Rha*p*	1.0 ± 0.58	–

tr = traces.
[a] 2,3,4,6-Galactose is 1,5-di-*O*-acetyl-2,3,4,6-tetra-*O*-methyl galactitol, etc..

the presence of 1 → 2 linkages in *A. senegal,* such as 1 → 2,3,6 Gal*p* instead of 1 → 3,6 Gal*p*. Furthermore, it is also interesting to note that the next abundant glycosidic linkages, in order of importance, differed between Acacia gums and could have important information about their structural differences. *A. senegal* gum contained a higher proportion of 1 → 3,4,6 Gal*p*, T-Rha*p*, T-Gal*p*, and 1 → 3,4 Gal*p*. In contrast, *A. seyal* contained more linear chains involving linkages such as 1 → 2 Ara*p*, 1 → 4 Gal*p*, 1 → 2 Ara*f*, and 1 → 6 Gal*p*. *A. senegal* also contained more non-reducing ends than *A. seyal* since the total content of residues in terminal position was higher in *A. senegal* (34.9%) than in *A. seyal* gum (16.6%).

To conclude, these results were consistent with the literature where it has been suggested that the common sugar-based structure of both Acacia gums is formed by a core structure of 1,3-linked β-D-Gal*p* chains substituted in position 6 by side chains of α-L-Ara*f*, β-D-Glc*p*A, and the following terminal disaccharides [Rha*p*-(1 → 4)-Glc*p*A]. However, beyond some similarities between gums, our results suggested that *A. senegal* was constituted by more terminal units and more ramified residues, thus a more branched structure, than *A. seyal*. In contrast, *A. seyal* displayed more linear residues of β-D-Gal*p*, α-L-Ara*p,* and α-L-Ara*f*, likely producing longer and less ramified branches in its structure than in the *A. senegal* structure. Similarly, it has previously been proposed that the structure of *A. seyal* was formed by long arabinosyl side chains in its polysaccharide structure (Nie et al., 2013b; Street & Anderson, 1983). In addition, the identification and the quantification of glycosidic linkages in *A. senegal* and A. *seyal* gums allowed the calculation of their branching degree (DB). Here, DB is defined as following: DB = 2D/(2D + L), where D is the number of dendritic units or branched units linked at three or more sites (e.g. 1 → 3,4 Gal*p*) and L is the number of linear units having two glycosidic linkages (e.g. 1 → 3 Gal*p*), respectively (Hölter, Burgath, & Frey, 1997). The calculated DB was 78.2% and 59.2% for *A. senegal* and *A. seyal*, respectively. Hence, this result confirmed that both gums are hyperbranched polysaccharides with more branched polysaccharidic architectures for *A. senegal* than for *A. seyal*.

3.2. Secondary structure

The secondary structure of Acacia gum polysaccharide-protein complex was probed by far UV-CD measurements between 190 and 260 nm (Fig. 1). *A. senegal* and *A. seyal* spectra displayed a strong decrease of ellipticity below 195 nm. It is well known that sugars as galactose and arabinose, of which both Acacia gums are mainly composed, absorb in this wavelength region (Homer, Roberts, Lane, & Nr, 1979; Listowsky, Englard, & Avigad, 1972; Listowsky & Englard, 1968). Moreover, Shpak, Barbar, Leykam, and Kieliszewski (2001) demonstrated the decrease of the ellipticity below 195 nm, with a minimum at 180 nm, when polysaccharide side chains were present on hydroxyproline-rich proteins. Therefore, the sharp decrease in ellipticity below 195 nm in *A. senegal* and *A. seyal* spectra was attributed to the substitution of the polypeptide backbone by polysaccharidic chains. Far UV-CD spectra also showed a minimum in ellipticity at 206 nm and a maximum at 228 nm for *A. seyal*, and a minimum at 210 nm and an inflection point at 227 nm for *A. senegal* gum. Among the secondary structures adopted by a protein, only helical conformations of the polyproline type II structure and unordered (random coil) protein conformations exhibit negative ellipticity near 200 nm (Brahms & Brahms, 1980; Woody, 1996). The CD spectrum of polyproline type II structures is characterised by a relatively weak positive band near 220 nm and a strong negative band near 200 nm (Woody, 1996). Hence, certainly both *A. senegal* and *A. seyal* gums were partially structured into polyproline type II helices, as previously found in *A. senegal* gum macromolecules (Renard et al., 2014, 2012, 2006), and in several hydroxyproline-rich glycoproteins (Perris et al., 2001; Shpak et al., 2001; Zhao et al., 2002). Despite these similarities in the global feature of both Acacia gums spectra, the negative minimum ellipticity at 210 nm in *A. senegal* gum was shifted left toward a lower wavelength value, from 210 to 206 nm, and increased in intensity in *A. seyal* gum spectrum. Furthermore, the maximum positive ellipticity, near 227 nm, was better defined in *A. seyal* than in *A. senegal*. These differences in ellipticity might reflect a higher polyproline type II helix content in *A. seyal* than in *A. senegal* gum. It is well known that the sugar composition, particularly the highest arabinose content, and the presence of long oligosaccharide side chains on the polypeptide backbone could promote the formation of polyproline type II helix. Shpak et al. (2001) evidenced that the presence of arabinosyl side chains on hydroxyproline-rich proteins favour the formation of polyproline type II helix while the addition of arabinogalactan polysaccharides side chains lead to a more random coil structure. The biochemical analyses of Acacia gums, showing higher total arabinose content (52 vs. 34 %mol) and more arabinosyl side chains linked to 2, 3, or 5 position (35 vs. 17.8 %mol) in *A. seyal* than in *A. senegal* were in good agreement with this statement. Therefore, it can be suggested that the polypeptidic part of *A. seyal* gum is certainly more structured with a higher polyproline type II helix content than that of *A. senegal* gum.

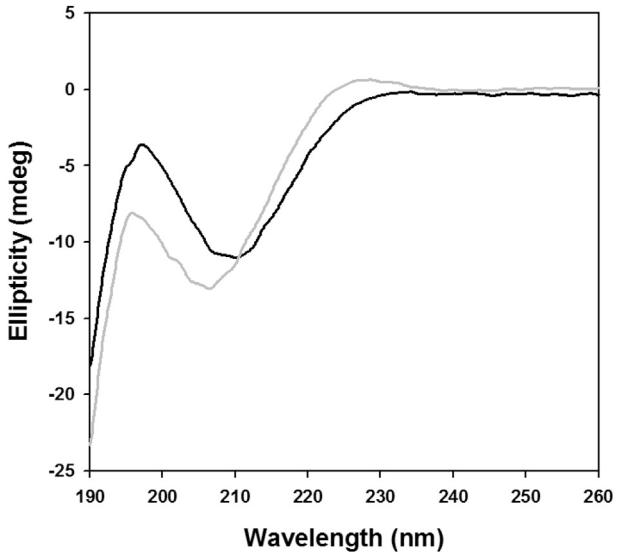

Fig. 1. Far-UV circular dichroism spectra of *A. senegal* (black) and *A. seyal* (gray) gums in aqueous solutions (Concentration of 2 %w/w at pH 5.0).

3.3. FTIR

FTIR spectra of *A. senegal* and *A. seyal* gums were acquired between 800 and 1900 cm^{-1} (Fig. 2). Acacia gums were analysed in solid state to avoid the strong contribution of water absorption, especially in the amide I band region (1720–1580 cm^{-1}) (Renard et al., 2006). FTIR spectra of both Acacia gums showed four main spectral bands in the wavenumber region between 1700 and 1200 cm^{-1} (Table 4, bands A-D). They could be partially attributed to the contribution of proteins in Acacia gums. In FTIR spectra of proteins, vibrations of amide I and amide II bands are located near 1650 and 1550 cm^{-1}, respectively. They mainly depends on the secondary structure of the polypeptide backbone and are hardly affected by the nature of the side chains (Barth, 2007; Barth & Zscherp, 2002). However, FTIR spectra of some polysaccharides

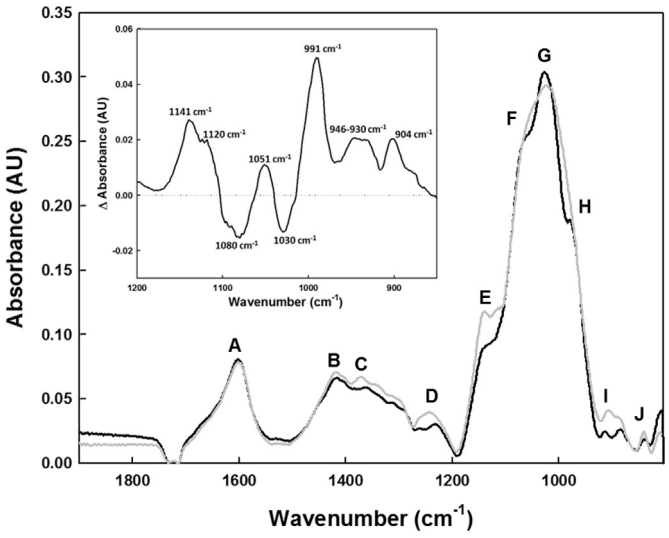

Fig. 2. Fourier transform infrared (FTIR) spectra of *A. senegal* (black) and *A. seyal* (gray) freeze-dried gums from 800 to 1900 cm^{-1}. Inset: spectral subtraction of *A. senegal* from *A. seyal* in the region from 850 to 1200 cm^{-1}.

containing uronic acids produced also some bands in this wavenumber region, towards 1740, 1620, and 1420 cm^{-1} (Boulet, Williams, & Doco, 2007; Manrique & Lajolo, 2002; Vinod & Sashidhar, 2010). The band position near 1620 cm^{-1} can move depending on the biochemical composition and particularly the content of uronic acids. Boulet et al. (2007) reported that the absorbance band of carboxylic functions of wine AGP's varied from 1640 to 1600 cm^{-1} when the uronic acid content increased from 3.6 to 14.7 % (Boulet et al., 2007). *A. senegal* and *A. seyal* gums were composed of a significant content of glucuronic acid and *4-O-Me*-glucuronic acid, 16.1%molar and 10.4%molar respectively, and a low content of proteins, 2.7% and 1.0% respectively. Therefore, absorbance bands at 1602 and 1416 cm^{-1} in *A. senegal* spectrum and bands at 1601 and 1420 cm^{-1} in *A. seyal* spectrum were mainly assigned to the absorbance of deprotonated carboxylic function of glucuronic acids (Boulet et al., 2007; Manrique & Lajolo, 2002) (Table 4, band A and B). Moreover, IR bands near 1360 and 1232 cm^{-1} in *A. senegal* spectrum and near 1370 and 1243 cm^{-1} in *A. seyal* spectrum might be caused by C–O–C stretching and C–H bending vibrations and deformations. These vibrations were hardly attributed to a specific functional group (Table 4, band C and D). Even thought, around this wavenumber region (1370–1230 cm^{-1}) previous works reported the contribution of proteins (Band amide III) (Barth & Zscherp, 2002), phenolic esters attached to polysaccharides (Séné, McCann, Wilson, & Grinter, 1994), and methyl ester groups (CH_3), which could come, for instance, from *4-O-Me*-glucuronic acids and proteins in Acacia gums (Barth, 2007; Synytsya, Copíková, Matejka, & Machovic, 2003).

The infrared spectral bands comprised in the wavenumber region between 1200 and 800 cm^{-1} had a more complex interpretation and corresponded to the carbohydrate moiety of Acacia gums (Table 4, band E-J). This so-called carbohydrate fingerprint region is produced by the skeletal stretching vibrations of the backbone and side chains of polysaccharides, and it is dominated by ring vibrations overlapped with stretching vibrations of (C–OH) side groups and (C–O–C) glycosidic bond vibrations (Kacuráková, Capek, Sasinková, Wellner, & Ebringerová, 2000). In this wavenumber region, the Acacia gum spectra were characteristic of spectra from other Acacia gum samples and polysaccharides rich in galactose and arabinose (PRAG's) (Boulet et al., 2007; Kacuráková et al., 2000; Renard et al., 2006). The maximal absorbance peaks were found at 1027 and 1023 cm^{-1} for *A. senegal* and *A. seyal*, respectively. The *A. senegal* peak displayed some lateral shoulders near 1160, 1140, and 974 cm^{-1} while the *A. seyal* lateral shoulders were near 1141 and 1050 cm^{-1}. Those spectral profiles were comparable with FTIR spectra of plant cell wall polysaccharides that had a similar composition than Acacia gums. In a previous study from Kacuráková et al. (2000), the main IR bands were reported between

Table 4
Characteristics of principal absorbance bands in Fourier Transform Infrared (FTIR) spectra of *A. senegal* and *A. seyal* gums with their corresponding vibrations and assignments according to literature. δ, γ, and *ν* correspond to in-plane bending, out-of-plane bending, and stretching vibrations, respectively.

Band	Band position *A. senegal*	Band position *A. seyal*	Associated vibrations	Possible band assignment
A	1602 cm^{-1}	1601 cm^{-1}	ν(C=O)	- ~1650 and 1550 cm^{-1}: Band Amide I and II from proteins, respectively (Barth & Zscherp, 2002; Barth, 2007).
B	1416 cm^{-1}	1420 cm^{-1}	γ(CN) δ(NH) $(CCN)_{deform.}$ ν(C=C) $\nu(COO^-)$	- 1640–1600 and 1420 cm^{-1}: Deprotonated carboxylic function (COO^-) from uronic acids (Boulet et al., 2007; Manrique & Lajolo, 2002).
C	1360 cm^{-1}	1370 cm^{-1}	$\delta(CH_3)$	- 1444, 1371, 975–978, and 923 cm^{-1}: Methyl ester groups (CH_3) in pectin (Synytsya et al., 2003).
D	1232 cm^{-1}	1243 cm^{-1}	$(CH)_{deform.}$ δ(CO) δ(NH) δ(C–O) $\delta(OH)_{COOH}$ ν(C–O–C) ν(CN)	- 1280 and 1220 cm^{-1}: Methyl ester groups (CH_3) in acetylated pectate (Synytsya et al., 2003). - 1280–1260 cm^{-1}: Phenolic esters from cell walls depending on the attached groups (Séné et al., 1994). - ~1230 cm^{-1}: Band amide III from proteins, depending on their secondary structure (Barth & Zscherp, 2002; Séné et al., 1994).
E	1140 cm^{-1}	1141 cm^{-1}	ν(C–O–C)	- Carbohydrate fingerprint region (Kacuráková et al., 2000).
F	1060 cm^{-1}	1050 cm^{-1}	ν(C–OH)	- 1155–1038 cm^{-1}: Galactan with the main chain of β1→6 Gal*p* (Kacuráková et al., 2000).
G	1027 cm^{-1} max.	1023 cm^{-1} max.	ν(C–O)	- 1141–1039 cm^{-1}: Arabinan with Ara*f* in the main and side chains (Kacuráková et al., 2000).
H	974 cm^{-1}	–	ν(C–C)	- 1139–985 cm^{-1}: Arabinogalactan with β1→3 Gal*p* main chain and side chains with α1→3 Ara*f* (8%) and β1→6 Gal*p* (92% total Gal) (Kacuráková et al., 2000).
I	920 cm^{-1}	910 cm^{-1}	$\nu(O–CH_3)$	
J	880 cm^{-1}	880 cm^{-1}	ν(C–O) $\rho(CH_3)$ $(C_1–H)_{deform.}$ δ(OH) δ(CCH) δ(COH) Rings	- 1140–975 cm^{-1}: Arabinogalacto-rhamnoglycan with the main chain formed by β1→6 Gal*p* (24%) and α1→4 Rha*p* (42%), and side chains with α-Ara*f* and α1→5 Ara*p* (34% total Ara) (Kacuráková et al., 2000). - 900–870 cm^{-1}: β-linkages between sugars units (Kacuráková et al., 2000; Matsuhiro, 1996; Yuen, Choi, Phillips, & Ma, 2009).

1155 and 1038 cm^{-1} when the main chain was formed only by β1→6 Gal*p* (100%), between 1141 and 1039 cm^{-1} when the main and side chain were formed by Ara*f* (100%), and between 1139 and 985 cm^{-1} with a maximum at 1078 cm^{-1} when α Ara*p*, α1→3 Ara*f* (8% total Ara) and β1→6 Gal*p* were linked to a main chain composed by β1→3 Gal*p* (92% total Gal) (Kacuráková et al., 2000). Therefore the main bands observed in this wavenumber of Acacia gum spectra likely corresponded to a combined contribution of the high content of galactose and arabinose present in the main and side chains of both gums. Moreover, when rhamnose was also present in the structure (β1→4 Rha*p* 42% and β1→6 Gal*p* 24% backbone with Ara*f* side chains 34%), IR bands shifted to a lower frequency between 1140 and 975 cm^{-1} with a maximum at 1049 cm^{-1} (Kacuráková et al., 2000). Hence, the rhamnose content in gums which is higher in *A. senegal* (16%) than in *A. seyal* gum (3%) also contributed to the spectral profile in the wavenumber region between 1200 and 925 cm^{-1}. In addition, differences in band intensity between gum spectra were evidenced by spectral subtraction of *A. senegal* from *A. seyal* in the region between 1200 and 850 cm^{-1} (Fig. 2 inset). Positive peaks such as 1141–1120, 1051, 991, 946–930, and 904 cm^{-1} were bands with higher intensity in *A. seyal* spectrum while negative peaks around 1080 and 1030 cm^{-1} were higher-intensity bands in *A. senegal* spectrum. The interpretation of these spectral differences is still complex due to the different composition and structure of gums. However, analysing the main differences between Acacia gums, we could suggest that positive bands around 1141–1120 and 991 cm^{-1} might be produced by the highest content of arabinosyl side chains in *A. seyal* with contribution of methyl groups from 4-*O*-*Me*-Glucuronic acid. Close to this hypothesis, previous studies from Kacurakova et al. (1994) found a strong correlation between the peak intensity at 1160 and 990 cm^{-1} and the contribution of arabinosyl side chains linked at the position O-3 in xylans. On the other hand, the negative peak at 1080 or 1030 cm^{-1} could be associated to the content of rhamnose in *A. senegal,* which is the main difference in composition between *A. senegal* (16%) and *A. seyal* (3%), Finally, at lower wavenumber, spectra displayed the characteristic "anomeric region" where low-intensity bands near 920 and 880 cm^{-1} for *A. senegal* and near 910 and 880 cm^{-1} for *A. seyal* (Table 4, band I and J) could be attributed to β-glycosidic linkages mainly present in galactopyranose units in both Acacia gums (Kacuráková et al., 2000).

In summary, FTIR results presented the fingerprint of *A. senegal* and *A. seyal* gums with the main spectral differences in agreement with their glycosidic linkage composition.

3.4. Molecular weight distribution and structural features

The HPSEC-MALLS chromatograms of *A. senegal* and *A. seyal* are shown in Fig. 3. The elution profiles of *A. senegal* and *A. seyal* gums (RI, LS, and UV signals) displayed the presence of three populations of macromolecules differing in their proportion (RI signal) and hydrodynamic volume. Similar chromatograms were shown in several studies using HPSEC coupled online to similar kind of detectors (Al-Assaf, Phillips, & Williams, 2005; Renard et al., 2006). The first population (eluted between 25.0 and 28.3 mL in UV signal) corresponding to macromolecules with high M_w was mainly composed of arabinogalactan-proteins (AGP) and glycoproteins (GP) fractions (Renard et al., 2014, 2012, 2006). The second one (eluted between 28.3 and 33.2 mL) was mainly composed by the arabinogalactan-peptide fraction (AG) with also glycoprotein macromolecules (GP) (Renard et al., 2014, 2012, 2006). The third one (eluted between 33.2 and 35.4 mL) contained both arabinogalactan-peptide (AG) and glycoprotein (GP) macromolecules (Renard et al., 2014, 2012, 2006). The M_w distributions (MWD) of *A. senegal* and *A. seyal* gums in function of the elution volume are

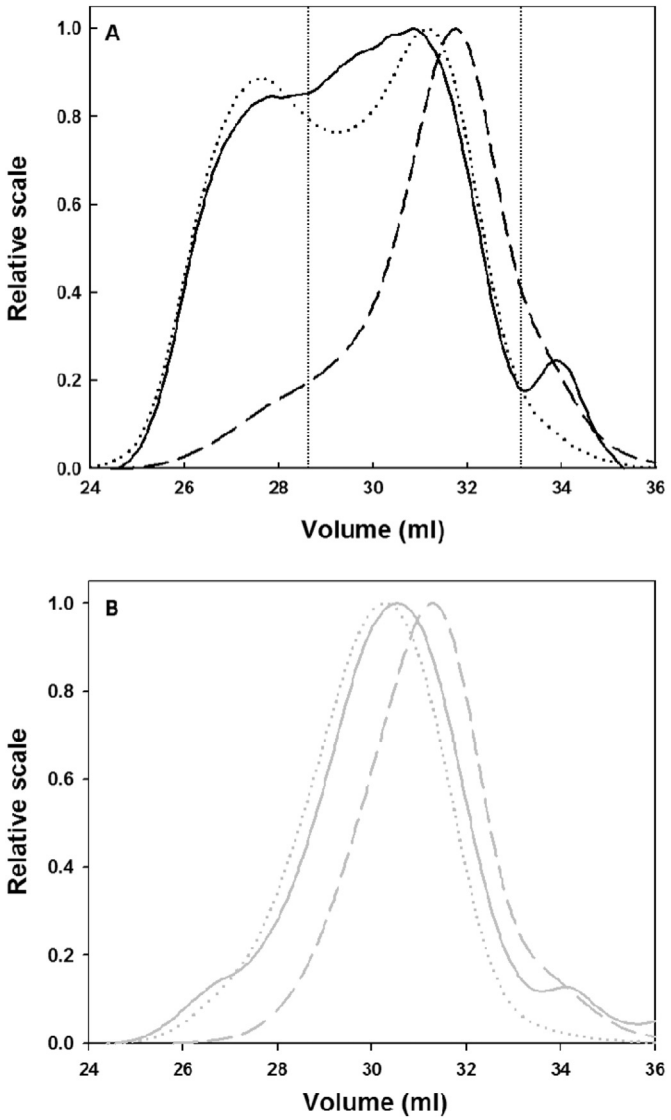

Fig. 3. High Performance Size Exclusion Chromatograms (HPSEC) showing the elution profiles of *A. senegal* (A) and *A. seyal* (B) gums monitored by differential refractive index (RI; dashed line), multi-angle laser light scattering (MALLS; dotted line), and UV at 280 nm (continuous line). Acacia gums were prepared in MilliQ water (Concentration of 1 g L^{-1} at pH 5) and eluted using 0.1 M $LiNO_3$ solution containing 0.02% NaN_3 as eluent. The *dn/dc* was 0.145 mL g^{-1}.

shown in Fig. 4. Along most of the elution volume, the MWD curve of *A. seyal* was located above that of *A. senegal*, except above 34–35 mL. The principle of size exclusion chromatography is based on the separation of macromolecules according to their hydrodynamic volume. Hence, for a same hydrodynamic volume (same elution volume), *A. seyal* macromolecules displayed higher M_w than *A. senegal* macromolecules suggesting a more compact structure of *A. seyal* macromolecules, as previously hypothesized (Al-Assaf et al., 2005).

The static (R_g, M_w, M_n) and dynamic ([η]) parameters were determined from HPSEC-MALLS chromatograms for *A. senegal* and *A. seyal* gums (Table 5). The R_g was measured but only considered for values above 10 nm, which is the sensitivity limit of the MALLS detector. Using this criterion, 50% of macromolecules for *A. senegal* gum and 30% for *A. seyal* gum were considered. *A. senegal* gum had a lower mean M_w (6.8×10^5 g mol^{-1}) than *A. seyal* gum (8.2×10^5 g mol^{-1}). On the contrary, the radius of gyration R_g and

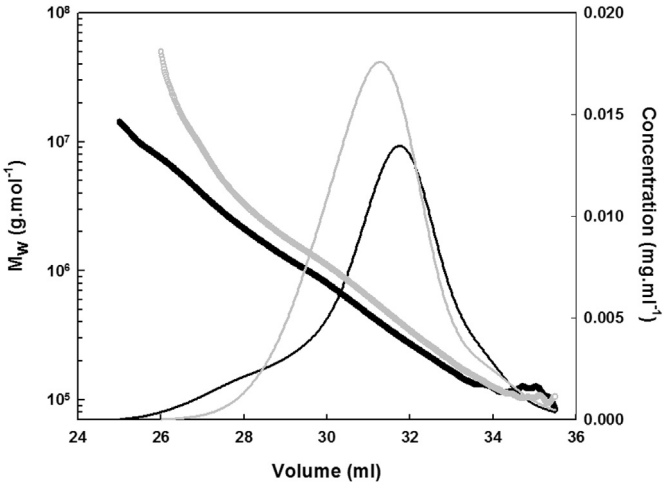

Fig. 4. Molecular weight distribution (M_w; thick line) and concentration profile (thin line) of *A. senegal* (black) and *A. seyal* (gray) gums prepared in aqueous solutions (Concentration of 1 g L^{-1} at pH 5).

the mean intrinsic viscosity [η] were higher for *A. senegal* (R_g: 30.8 nm; [η]: 22.8 mL g^{-1}) than for *A. seyal* gum (R_g: 17.1 nm [η]: 16.5 mL g^{-1}). The polydispersity index (M_w/M_n) was respectively 2.0 and 1.5 for *A. senegal* and *A. seyal* gums highlighting a higher proportion of high molecular mass macromolecules in *A. senegal* gum than in *A. seyal* gum. Similar mean parameters can be found in literature for both gums with small differences between them, probably due to the natural origin of gums and variations of experimental conditions (Al-Assaf et al., 2005; Idris et al., 1998; Renard et al., 2006; Sanchez, Renard, Robert, Schmitt, & Lefebvre, 2002). The differences observed in the structural parameters between both Acacia gums, particularly the highest mean M_w of *A. seyal* with the lowest mean R_g and [η], confirmed the highest compactness of *A. seyal* macromolecules. This more compact conformation cannot be explained by the degree of branching. It has to be understood as the consequence of smaller charge density in *A. seyal* macromolecules (then less intra-chain electrostatic repulsions), lower amino acid content (then less distance between sugar blocks), as well as the presence of long flexible arabinosyl chains likely able to self-organize and interact between them through hydrogen bonding or steric attraction. In addition, other effects such as the specific geometrical constraints between sugar blocks with a high chain density and the most structured polypeptide backbone can partially explain the largest compactness of *A. seyal* macromolecules.

To go deeper in the analysis of the structural features of Acacia gums, R_g vs M_w and [η] vs M_w plots were analysed. In general, R_g and [η] are related to the molecular weight as a simple power law relationship according to $R_g = K_g M_w^{\nu g}$ and $[\eta] = K_\alpha M_w^{\alpha}$ where the parameters K_g and K_α are the corresponding constants (Burchard, 1999). In the present paper, only the exponent values ν_g and α, called static and hydrodynamic coefficients, will be considered and compared to theoretical values to gain some insights into the shape of the studied macromolecules. Exponent values depend on the overall shape of polymers, especially anisotropy, temperature, and polymer–solvent interactions that determines the chain density of polymers. It is important to recall that these power law relationships are strictly valid only for macromolecules with monodisperse M_w. Since each point of the plots was measured on a low volume elution slice, the polydispersity index of each sample was lower than 1.1. Then the analysis can be performed at least in a qualitative way. The log–log plot of R_g vs M_w is shown in Fig. 5 for both Acacia gums. The first remark is that plots cannot be described by a single slope, demonstrating the presence of biopolymers with different conformations and/or density. These deviations from an unique power law behaviour on the whole studied M_w range are reminiscent of hyperbranched macromolecules due to their different branching density and/or length of branches (Ioan, Aberle, & Burchard, 2000; Rolland-Sabaté, Colonna, Mendez-Montealvo, & Planchot, 2007; Rolland-Sabaté, Mendez-Montealvo, Colonna, & Planchot, 2008), but also to different biopolymer anisotropy. The plot for *A. senegal* displayed two slopes with a value of 0.63 in the lowest M_w range (3.55×10^5–2.56×10^6 g mol^{-1}; 44% of macromolecules) and 0.51 in the highest M_w range (2.56×10^6–9.95×10^6 g mol^{-1}; 4% of macromolecules) (Table 6). It is difficult to compare our results with the few published ν_g values for *A. senegal* gum and their molecular fractions since only one slope was considered (Table 7). However, our exponent values were in the range of reported values comprised between 0.33 (M_w range: 3×10^6–6×10^6 g mol^{-1}; Flow Field Fractionation chromatography) and 1.2 (M_w range: 3×10^5–1×10^6 g mol^{-1}: HPSEC-MALLS). Based on theoretical ν_g values for spheres (0.33), linear

Table 5
Structural parameters of *A. senegal* and *A. seyal* gums in aqueous solutions (Concentration of 1 g L^{-1} at pH 5) obtained by HPSEC-MALLS using a *dn/dc* of 0.145 (mean ± standard deviation).

Structural parameters	*A. senegal*	*A. seyal*
M_w (g mol^{-1})	$6.8 \times 10^5 \pm 8.1 \times 10^3$	$8.2 \times 10^5 \pm 3.2 \times 10^3$
M_n (g mol^{-1})	$3.4 \times 10^5 \pm 8.6 \times 10^3$	$5.3 \times 10^5 \pm 1.7 \times 10^4$
M_w/M_n	2.0 ± 0.07	1.5 ± 0.05
R_g (nm)	30.8 ± 0.6	17.1 ± 0.4
[η] (mL g^{-1})	22.8 ± 0.20	16.5 ± 0.4

M_w: weight-average molecular mass. M_n: number-average molecular mass. M_w/M_n: polydispersity index. R_g: gyration radius (>10 nm). [η]: intrinsic viscosity.

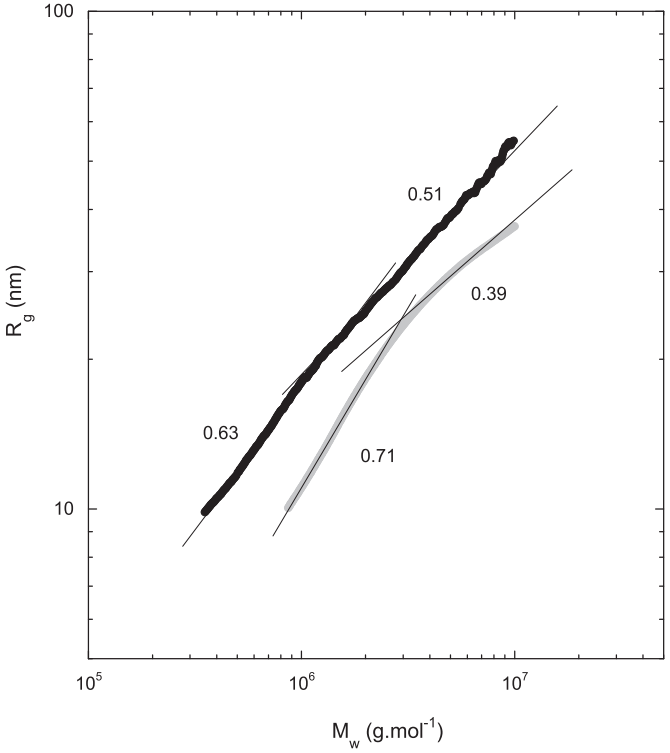

Fig. 5. Radius of gyration (R_g) as a function of molecular weight (M_w) for *A. senegal* (black) and *A. seyal* (gray) gums prepared in MilliQ water (Concentration of 1 g L^{-1} at pH 5). ν_g values were calculated from the relation $R_g = K_g M_w^{\nu g}$.

Table 6
Exponents ν_g and α calculated from the relation $R_g = K_g M_w^{\nu g}$ and $[\eta] = K_\alpha M_w^{\alpha}$ for *A. senegal* and *A. seyal* gums prepared in aqueous solutions (Concentration of 1 g L^{-1} at pH 5).

Exponent	Type of gum	Value	M_w range (g mol^{-1})	Fraction of macromolecules (%)
ν_g	*A. senegal*	0.63	3.55×10^5–2.56×10^6	44.4
		0.51	2.56×10^6–9.95×10^6	4.2
	A. seyal	0.71	8.65×10^5–2.77×10^6	27.5
		0.39	2.77×10^6–9.98×10^6	2.0
α	*A. senegal*	0.44	1.26×10^5–5.37×10^5	64.8
		0.78	5.42×10^5–1.25×10^6	19.1
		0.44	1.26×10^6–9.90×10^6	11.5
	A. seyal	0.28	1.50×10^5–6.30×10^6	96.2

random coils (between 0.5 and 0.6 depending on the solvent quality). and rods (1) (Burchard, 1999), it was tempting to ascribe the found exponent values to the presence of more or less extended linear random coils. However, such conclusion would be misleading because it was demonstrated that Acacia gum macromolecules are hyperbranched polymers. In addition, polymers with different shapes can display similar ν_g exponent values. For instance, a value of 0.5 can be found for linear random coils in Θ-conditions, thin discs, non-swollen randomly branched polymers, and star molecules in Θ-conditions (Burchard, 1994). Another feature to take into account is that hyperbranched macromolecules having different architectures, the same hydrodynamic volume but not necessarily the same M_w may co-elute (Gaborieau, Gilbert, Gray-Weale, Hernandez, & Castignolles, 2007; Li, Lu, An, & Wu, 2013; Vilaplana & Gilbert, 2010). In the best-case scenario, polymers can be described in terms of anisotropy and chain density depending on the ν_g exponent values, except if complementary structural information is available. Since it was previously evidenced that all biopolymers from *A. senegal* gum exhibit oblate or triaxial ellipsoid shapes (Renard et al., 2014, 2012; Sanchez et al., 2008); therefore, the ν_g exponents for *A. senegal* gum were likely due to the ellipsoidal shapes of macromolecules which were indeed quite close to the thin disc theoretical ν_g. Similarly, hyperbranched polysaccharides with oblate ellipsoidal shape such as amylopectin from starch displayed ν_g exponent values comprised between 0.3 and 0.6 (Lelievre, Lewis, & Marsden, 1986; Roger, Bello-Perez, & Colonna, 1999; Rolland-Sabaté et al., 2007).

The R_g vs M_w plot for *A. seyal* gum (Fig. 5) displayed also two slopes with ν_g exponent values of 0.71 (low M_w range; 28% of macromolecules) and 0.39 (high M_w range; 2% of macromolecules), not so different from those previously obtained for *A. senegal* gum in quite similar M_w ranges (Table 6). It was not possible to compare our results with previous ones since no literature data exists for *A. seyal* gum. Nevertheless, it can be noticed that the average exponent value was again around 0.5, suggesting that the global conformation of *A. seyal* macromolecules could be ellipsoidal, and that the ν_g values decreased when increasing the M_w range. Similar trend can be observed for *A. senegal* gum in Table 6 suggesting that larger macromolecules were more compact or/and less anisotropic than smaller ones. Alternatively, very small exponent values around or below 0.3 can also indicate the presence of aggregates (Bello-Perez, Roger, Colonna, & Paredes-Lopez, 1998). From our experience, above a M_w of about $2–3 \times 10^6$ g mol^{-1}, aggregates of Acacia gum polymers are always present in solution. Other hyperbranched polysaccharides such as glycogen from rabbit liver or mussels can display different exponent values depending on their M_w, with values comprised between 0.40-0.74 in the low M_w region and 0.30–0.40 in the high M_w regions (Ioan, Aberle, & Burchard, 1999; Rolland-Sabaté et al., 2007). As well, highly branched dextran can also display lower exponent value at higher M_w (Rolland-Sabaté et al., 2008).

The analysis of Acacia gums using the Mark-Houwink-Sakurada (MHS) relationship, $[\eta]$ vs M_w, gave further information on the conformation and structure of macromolecules since more than 95% of macromolecules were concerned by the analysis. The α power law exponent values theoretically range from 0 (sphere) to 1.8 (rod) with 0.5–0.8 intermediate values for flexible polymers depending on the solvent quality (S. B. Ross-Murphy, 1994). However, like for the ν_g exponent, macromolecular conformation analyses from α values has to be done carefully because of molecular polydispersity, effect of chain branching, and complex hydrodynamics (S. B. Ross-Murphy, 1994). MHS plot of both Acacia gums are given in Fig. 6. *A. seyal* MHS plot displayed one slope with α exponent value of 0.28, suggesting a homogeneous distribution of macromolecule hydrodynamic volumes (Table 6). On the other hand, *A. senegal* MHS plot clearly displayed three slopes with α exponent values of 0.44, 0.78, and 0.44 for macromolecules with M_w below 5.4×10^5 g mol^{-1}, M_w between 5.4×10^5 and 1.3×10^6 g mol^{-1}, and above 1.3×10^6 g mol^{-1}, respectively (Table 6 & Fig. 6). This indicates that macromolecules with M_w on the intermediate range displayed larger anisotropy or smaller chain density than those in the low and high accessible M_w range. The average α value was 0.55, a value close to those found in the literature (Table 7). Our data mainly indicated that *A. seyal*

Table 7
. Exponents ν_g and α obtained from the relation $R_g = K_g M_w^{\nu g}$ and $[\eta] = K_\alpha M_w^{\alpha}$ and the anisotropy parameter ρ (R_g/R_v) for *A. senegal* gum according to the literature.

M_w region ($\times 10^{-3}$ g mol^{-1})	ν_g	α	ρ (=R_g/R_h)	References
120–6000		0.55	1.20	(Sanchez et al., 2002)
		0.51–0.55		(Masuelli, 2013)
340 (average)			1.5–3.5 (mean: 2.7)	(Alftrén, Peñarrieta, Bergenståhl, & Nilsson, 2012)
1900 (average)			1.1–1.5 (mean: 1.2)	(Alftrén et al., 2012)
3000–6000	0.33		0.6–0.9	(Picton, Bataille, & Muller, 2000)
300–1000	1.18			(Aoki, Al-Assaf, Katayama, & Phillips, 2007)
1000–100000	0.41			(Aoki et al., 2007)
500–1100	0.63			(Wang, Burchard, Cui, Huang, & Phillips, 2008)
		0.54		(Anderson & Rahman, 1967)
400–2500		0.55		(Vandevelde & Fenyo, 1985)
500–2000	0.42		0.6–1.3	(Idris et al., 1998)

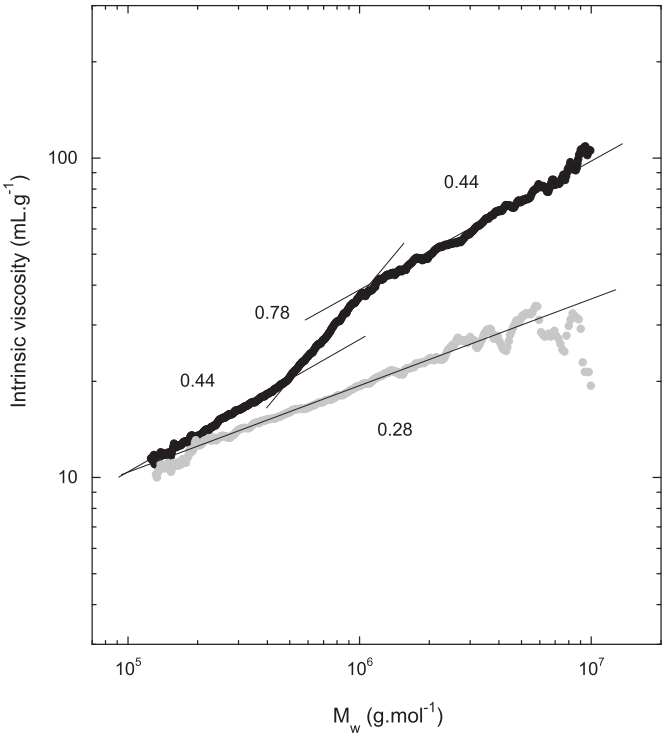

Fig. 6. Mark-Houwink-Sakurada (MHS) plot for *A. senegal* (black) and *A. seyal* (gray) gums prepared in MilliQ water (Concentration of 1 g L^{-1} at pH 5) showing the intrinsic viscosity ([η]) as a function of molecular weight (M_w). α exponent values were calculated from the relation $[\eta] = K_\alpha M_w^{\alpha}$.

macromolecules adopted more compact conformation in water than *A. senegal* macromolecules, as above mentioned. In literature, hyperbranched polysaccharides such as amylopectin, dextran, or glycogen exhibit α exponent values around 0.3–0.5 (Callaghan & Lelievre, 1985; Lelievre et al., 1986; Millard, Dintzis, Willett, & Klavons, 1997; Rolland-Sabaté et al., 2008). Similar results were obtained with synthetic hyperbranched polymers with finely tuned structural characteristics (Li et al., 2013). The theory on branched polymers and the recent numeric simulation on flexible polymers demonstrated that hyperbranching decreases the α exponent below 0.5, and a branching degree higher than 0.5 gave lower α values in the high M_w range than in the low range (Aerts, 1998; Lu, An, & Wang, 2013; Tao, Zhang, Yan, & Wu, 2007). Based on the sole effect of branching density on α exponent, and assuming identical all other structural parameters, smaller α values were expected for the most branched *A. senegal* gum. However, results found exactly the opposite. As suggested before, differences in composition between Acacia gums might influence the conformation of gum macromolecules. The specific sugar composition of *A. seyal* gum, especially the lowest concentration of charged sugars and the highest content of long arabinose side chains distributed among sugar blocks and polypeptide architectures with plasticising properties can promote a more compact conformation, then a smaller α exponent for *A. seyal* macromolecules than for *A. senegal* macromolecules.

Another way to consider static (R_g) and hydrodynamic ([η]) parameters determined from HPSEC-MALLS experiments is to combine them calculating the so called ρ structural parameter by the R_g/R_h ratio (Burchard, 1999). To calculate ρ, we first calculate the sphere equivalent intrinsic viscosity-based hydrodynamic radius (R_h) according to the equation $R_h = (3[\eta]M_w/10\pi N_a)$, where N_a is the Avogadro number (Tanford, 1979). The R_h calculated from [η] can be slightly different from R_g measured by dynamic light scattering and the ratio between them increases with polymer anisotropy, being comprised between 1 and 1.1 for circular cylinders or triaxial ellipsoids (Li et al., 2013; Mansfield & Douglas, 2013). The ρ structural parameter is also named the asymmetry (Adolphi & Kulicke, 1997) or anisotropy parameter (Mansfield & Douglas, 2013). It depends on the chain architecture and conformation of macromolecules, and it is known to be affected by the macromolecular flexibility and polydispersity (Adolphi & Kulicke, 1997). Theoretical ρ values are 0.778 for hard homogeneous spheres, 0.977 for dendrimers equivalent to Gaussian soft spheres, and between 1.08 and 1.33 for regular stars with many uniform-length chains. Hyperbranched polymers or regular stars with numerous polydisperse arms have ρ values of 1.22 and from 1.5 to 1.73 for random coil and linear chains, the last ones increasing their values close to 2 in good solvent conditions (Burchard, 1999). It was clearly observed from these theoretical values that the ρ parameter depends on polymer anisotropy and values between 1 and 1.3 are usually found for branched and hyperbranched polymers. However, it is obviously impacted by the global polymer density through the R_g term (Adolphi & Kulicke, 1997) and more specifically by the polymer inhomogeneity (Mansfield & Douglas, 2013).

The plot of ρ vs M_w for *A. senegal* and *A. seyal* gums is shown in Fig. 7. Curves encompass 50% of macromolecules for *A. senegal* gum and 30% for *A. seyal*. Although variations were small, the ρ parameter of both Acacia gums was not constant in the considered M_w range. For *A. senegal* gum, ρ values were first constant at 1.02 up to a M_w of 10^6 g mol^{-1}, they increased from 1.02 to 1.2 ($M_w \sim 3 \times 10^6$ g mol^{-1}), and then they remained constant. For *A. seyal*, all ρ values were lower than those for *A. senegal* gum. They increased from 0.75 to 1.02 ($M_w < 5 \times 10^6$ g mol^{-1}), and then they did not evolve. Similarly, previous works on *A. senegal* gum have shown that ρ increases with the M_w (Table 7), and this trend was also observed with purified fractions (Renard et al., 2014, 2012;

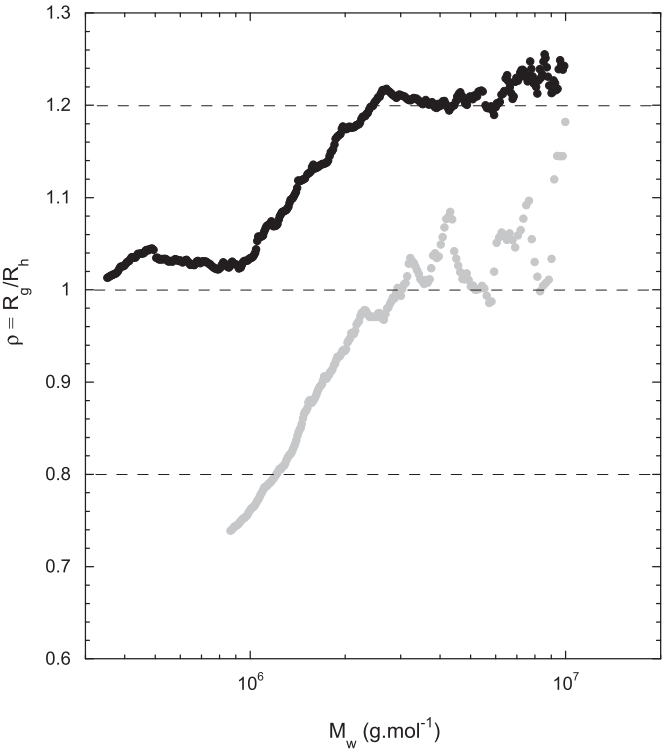

Fig. 7. The ρ structural parameter (R_g/R_h) as a function of molecular weight (M_w) for *A. senegal* (black) and *A. seyal* (gray) gums prepared in MilliQ water (Concentration of 1 g L^{-1} at pH 5).

Sanchez et al., 2008). These previous results are in line with our own data. Depending on the M_w, ρ values of both Acacia gums are compatible with the presence of more or less dense hyperbranched architectures with spheroidal, oblate ellipsoidal or triaxial ellipsoidal conformations (Burchard, 1999; Ioan et al., 1999, 2000; Lelievre et al., 1986; Matsuoka et al., 2006; Renard et al., 2014, 2012; Rolland-Sabaté et al., 2008; Sanchez et al., 2008). For both Acacia gums, the increase of ρ values with M_w could be promoted either by the increase of macromolecules anisotropy or/and by the decrease of their density. In order to differentiate anisotropy from density effects, some authors calculated the apparent density of macromolecules according to the following relationship based on an equivalent sphere: $d_{app} = (M_w/N_a)/(4/3\pi R_g^3)$ (Adolphi & Kulicke, 1997; Rolland-Sabaté et al., 2008). The apparent density of macromolecules from both gums decreased with M_w suggesting that *A. seyal* macromolecules were denser than those of *A. senegal* gum (results not shown). The increase of the ρ parameter with M_w is mainly due to the presence of larger macromolecules (or aggregates of macromolecules) being more anisotropic. A way to check this assumption is to plot R_g vs R_h and to compare experimental data with theoretical calculations of objects with increasing anisotropy, usually sphere, oblate and prolate ellipsoids, and rods (Adolphi & Kulicke, 1997; Matsuoka et al., 2006; Van de Sande & Persoons, 1985; Young, Missel, Mazer, Benedek, & Carey, 1978). Fig. 8 clearly shows that macromolecules from *A. seyal* displayed spheroidal conformations at low M_w (small R_g and R_h) while more anisotropic conformations close to oblate ellipsoids at larger M_w (higher R_g and R_h). In contrast, *A. senegal* macromolecules adopted oblate ellipsoid-like conformations at low M_w, which was confirmed elsewhere (Sanchez et al., 2008), and more anisotropic conformations at larger M_w, varying between oblate and prolate ellipsoids, as demonstrated recently (Renard et al., 2014, 2012).

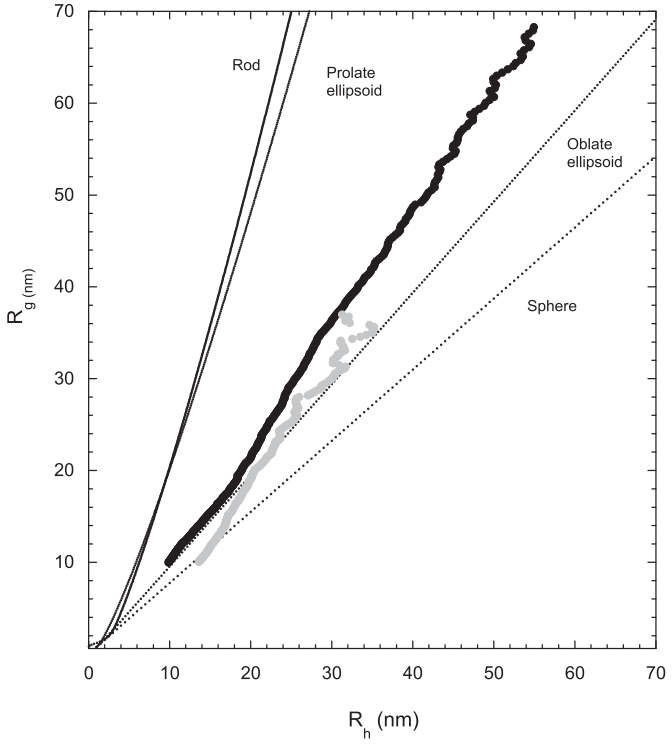

Fig. 8. Radius of gyration (R_g) as a function of hydrodynamic radius (R_h) for *A. senegal* (black) and *A. seyal* (gray) gums prepared in MilliQ water (Concentration of 1 g L^{-1} at pH 5) and compared with theoretical calculations for objects with increasing anisotropy going from sphere, oblate ellipsoid, prolate ellipsoids, and rods.

4. Conclusions

This work aimed to characterize the biochemical and structural properties of *A. senegal* and *A. seyal* gums producing a complete overview of their intrinsic features. These two Acacia gums are hyperbranched polysaccharides rich in arabinose and galactose (PRAG). They showed some similarities in their global biochemical and structural properties, as well as differences that were determinants for their macromolecular conformation. The *A. senegal* macromolecules, the richest in charged acidic sugars and proteins, had more branched global architectures than *A. seyal* macromolecules. Both Acacia gums were structured into polyproline type II helices. *A. senegal* gum was more polydisperse than *A. seyal* gum with the highest proportion of high molecular mass macromolecules. *A. seyal* macromolecules were more structured and compact than *A. senegal* ones presenting the lowest intrinsic viscosity. For both Acacia gums, the anisotropy of macromolecules increased with the increase of the molecular weight. The conformation of *A. seyal* macromolecules varied from spheres to oblate ellipsoids while *A. senegal* macromolecules varied from oblate ellipsoids to more anisotropic conformations, such as oblate and prolate ellipsoids.

In order to relate the characterisation of Acacia gums covered in this paper to their physicochemical properties, we have planned to compare hydration, rheological, and interfacial properties of *A. senegal* and *A. seyal* gums. Since, currently, both Acacia gums are almost equal in industrial relevance, a complete description of both Acacia gums becomes a key tool for a better understanding of gum quality determinants, leading a better selection, use, and control of gums for specific applications.

Acknowledgements

The authors would thank ALLAND & ROBERT Company – Natural and organic gums (Port Mort, France) and the French Ministry of Research and Education (2012/ 0157) for financial support (Ph.D. D. L. Lopez-Torrez).

References

Adolphi, U., & Kulicke, W. M. (1997). Coil dimension and conformation of macromolecules in aqueous media from flow field-flow fractionation/multi-angle laser light scattering illustrated by studies on pullulan. *Polymer, 38*, 1513–1519.
Aerts, J. (1998). Prediction of intrinsic viscosities of dendritic, hyperbranched and branched polymers. *Computational and Theoretical Polymer Science, 8*, 49–54.
Akiyama, Y., Eda, S., & Kato, K. (1984). Gum Arabic is a kind of arabinogalactan protein. *Agricultural and Biological Chemistry, 48*(1), 235–237.
Al-Assaf, S., Andres-Brull, M., Cirre, J., & Phillips, G. O. (2012). Structural changes following industrial processing of Acacia gums. In *Gum arabic* (pp. 153–168). The Royal Society of Chemistry. http://dx.doi.org/10.1039/9781849733106-00153.
Al-Assaf, S., Phillips, G., & Williams, P. (2005). Studies on acacia exudate gums. Part I: the molecular weight of gum exudate. *Food Hydrocolloids, 19*(4), 647–660. http://dx.doi.org/10.1016/j.foodhyd.2004.09.002.
Al-Assaf, S., Sakata, M., McKenna, C., Aoki, H., & Phillips, G. O. (2009). Molecular associations in acacia gums. *Structural Chemistry, 20*(2), 325–336. http://dx.doi.org/10.1007/s11224-009-9430-3.
Albersheim, P., Nevins, D. J., English, P. D., & Karr, A. (1967). A method for the analysis of sugars in plant cell wall polysaccharides by gas-liquid-chromatography. *Carbohydrate Research, 5*, 340–345.
Alftrén, J., Peñarrieta, J. M., Bergenståhl, B., & Nilsson, L. (2012). Comparison of molecular and emulsifying properties of gum arabic and mesquite gum using asymmetrical flow field-flow fractionation. *Food Hydrocolloids, 26*(1), 54–62.
Anderson, D. M. W. (1966). Studies on uronic acid materials. *Carbohydrate Research, 2*, 104–114.
Anderson, D. M. W., & Rahman, S. (1967). Studies on uronic acid materials. *Carbohydrate Research, 4*(4), 298–304.

Anderson, D. M. W., Bridgeman, M. M. E., & De Pinto, G. (1984). Acacia gum exudates from species of the series gummiferae. *Phytochemistry, 23*(3), 575–577. http://dx.doi.org/10.1016/S0031-9422(00)80383-0.

Anderson, D. M. W., & Farquhar, J. G. K. (1979). The composition of eight Acacia gum exudates from the series Gummiferae and Vulgares. *Phytochemistry, 18*(4), 609–610. http://dx.doi.org/10.1016/S0031-9422(00)84269-7.

Anderson, D. M. W., Hirst, E., & Stoddart, J. F. (1966). Studies on uronic acid materials Part XVII some structural features of *Acacia senegal* gum (gum arabic). *Journal of the Chemical Society C: Organic*, 1959–1966.

Anderson, D. M. W., & McDougall, F. J. (1987). The amino acid composition and quantitative sugar-amino acid relationships in sequential Smith-degradation products from gum arabic (*Acacia senegal* (L.) Willd.). *Food Additives and Contaminants, 4*(2), 125–132. http://dx.doi.org/10.1080/02652038709373623.

Anderson, D. M. W., & Stoddart, J. F. (1966). Studies on uronic acid materials Part XV. The use of molecular-sieve chromatography in studies on *Acacia senegal* gum/Gum arabic). *Carbohydrate Research, 2*, 104–114.

Aoki, H., Al-Assaf, S., Katayama, T., & Phillips, G. O. (2007). Characterization and properties of Acacia senegal (L.) Willd. var. senegal with enhanced properties (Acacia (sen) SUPER GUM™): Part 2—Mechanism of the maturation process. *Food Hydrocolloids, 21*(3), 329–337.

Aspinall, G. O., & Fairweather, R. M. (1965). Araucaria bidwilli GUM. *Carbohydrate Research, 1*, 83–92.

Barth, A. (2007). Infrared spectroscopy of proteins. *Biochimica et Biophysica Acta, 1767*(9), 1073–1101. http://dx.doi.org/10.1016/j.bbabio.2007.06.004.

Barth, A., & Zscherp, C. (2002). What vibrations tell about proteins. *Quarterly Reviews of Biophysics, 35*(4), 369–430. http://dx.doi.org/10.1017/S0033583502003815.

Bello-Perez, L. A., Roger, P., Colonna, P., & Paredes-Lopez, O. (1998). Laser light scattering of high amylose and high amylopectin materials, stability in water after microwave dispersion. *Carbohydrate Polymers, 37*, 383–394.

Boulet, J. C., Williams, P., & Doco, T. (2007). A fourier transform infrared spectroscopy study of wine polysaccharides. *Carbohydrate Polymers, 69*(1), 79–85. http://dx.doi.org/10.1016/j.carbpol.2006.09.003.

Brahms, S., & Brahms, J. (1980). Determination of protein secondary structure in solution by vacuum ultraviolet circular dichroism. *Journal of Molecular Biology, 138*, 149–178.

Burchard, W. (1994). Light scattering techniques. In S. B. Ross-Murphy (Ed.), *Physical techniques for the study of food biopolymers* (pp. 151–213). Blackie Academic & Professional. http://dx.doi.org/10.1007/978-1-4615-2101-3_4.

Burchard, W. (1999). Solution properties of branched macromolecules. *Advances in Polymer Science, 143*, 113–194.

Callaghan, P. T., & Lelievre, J. (1985). The size and shape of amylopectin: a study using pulsed-field gradient nuclear magnetic resonance. *Biopolymers, 24*(3), 441–460. http://dx.doi.org/10.1002/bip.360240303.

Chikamai, B. N., Banks, W. B., Anderson, D. M. W., & Weiping, W. (1996). Processing of gum arabic and some new opportunities. *Food Hydrocolloids, 10*(3), 309–316. http://dx.doi.org/10.1016/S0268-005X(96)80006-3.

Churms, S. C., Merrifield, E. H., & Stephen, A. M. (1983). Some new aspects of the molecular structure of *Acacia senegal* gum (gum arabic). *Carbohydrate Research, 123*, 267–279.

Doco, T., O'Neill, M., & Pellerin, P. (2001). Determination of the neutral and acidic glycosyl-residue compositions of plant polysaccharides by GC-EI-MS analysis of the trimethylsilyl methyl glycoside derivatives. *Carbohydrate Polymers, 46*(3), 249–259. http://dx.doi.org/10.1016/S0144-8617(00)00328-3.

Doco, T., Williams, P., & Cheynier, V. (2007). Effect of flash release and pectinolytic enzyme treatments on wine polysaccharide composition. *Journal of Agricultural and Food Chemistry, 55*(16), 6643–6649. http://dx.doi.org/10.1021/jf071427t.

Ellis, M., Egelund, J., Schultz, C. J., & Bacic, A. (2010). Arabinogalactan-proteins: key regulators at the cell surface? *Plant Physiology, 153*(2), 403–419. http://dx.doi.org/10.1104/pp.110.156000.

FAO.. (1999). *Gum arabic*. Food and Nutrition Paper No 52, Addendum 7. Rome.

Flindt, C., Al-Assaf, S., Phillips, G. O., & Williams, P. A. (2005). Studies on acacia exudate gums. Part V. Structural features of *Acacia seyal*. *Food Hydrocolloids, 19*(4), 687–701. http://dx.doi.org/10.1016/j.foodhyd.2004.09.006.

Gaborieau, M., Gilbert, R. G., Gray-Weale, A., Hernandez, J. M., & Castignolles, P. (2007). Theory of multiple-detection size-exclusion chromatography of complex branched polymers. *Macromolecular Theory and Simulations, 16*(1), 13–28. http://dx.doi.org/10.1002/mats.200600046.

Gaspar, Y., Johnson, K. L., McKenna, J. A., Bacic, A., & Schultz, C. J. (2001). The complex structures of arabinogalactan-proteins and the journey towards understanding function. In N. C. Carpita, M. Campbell, & M. Tierney (Eds.), *Plant cell walls* (pp. 161–176). Netherlands: Springer. http://dx.doi.org/10.1007/978-94-010-0668-2_10.

Goodrum, L. J., Patel, A., Leykam, J. F., & Kieliszewski, M. J. (2000). Gum arabic glycoprotein contains glycomodules of both extensin and arabinogalactan-glycoproteins. *Phytochemistry, 54*, 99–106.

Harris, P. J., Henry, R. J., Blakeney, A. B., & Stone, B. A. (1984). An improved procedure for the methylation analysis of oligosaccharides and polysaccharides. *Carbohydrate Research, 127*(1), 59–73.

Hölter, D., Burgath, A., & Frey, H. (1997). Degree of branching in hyperbranched polymers. *Acta Polymerica, 48*(1–2), 30–35. http://dx.doi.org/10.1002/actp.1997.010480105.

Homer, R., Roberts, K., Lane, C., & Nr, N. (1979). Glycoprotein conformation in plant cell walls. *Planta, 146*, 217–222.

Idris, O. H. M., Williams, P. A., & Phillips, G. O. (1998). Characterisation of gum from *Acacia senegal* trees of different age and location using multidetection gel permeation chromatography. *Food Hydrocolloids, 12*(4), 379–388. http://dx.doi.org/10.1016/s0268-005x(98)00058-7.

Ioan, C. E., Aberle, T., & Burchard, W. (1999). Solution properties of glycogen. 1. Dilute solutions. *Macromolecules, 32*(22), 7444–7453. http://dx.doi.org/10.1021/ma990600m.

Ioan, C. E., Aberle, T., & Burchard, W. (2000). Structure properties of dextran. 2. Dilute solution. *Macromolecules, 33*(15), 5730–5739. http://dx.doi.org/10.1021/ma000282n.

Islam, A., Phillips, G., Sljivo, A., Snowden, M., & Williams, P. (1997). A review of recent developments on the regulatory, structural and functional aspects of gum arabic. *Food Hydrocolloids, 11*(4), 493–505. http://dx.doi.org/10.1016/S0268-005X(97)80048-3.

Kacuráková, M., Capek, P., Sasinková, V., Wellner, N., & Ebringerová, A. (2000). FT-IR study of plant cell wall model compounds: pectic polysaccharides and hemicelluloses. *Carbohydrate Polymers, 43*, 195–203.

Kennedy, J., Phillips, G., & Williams, P. (2010). *Gum arabic* (p. 333). RSC Publishing.

Lelievre, J., Lewis, J. A., & Marsden, K. (1986). The size and shape of amylopectin: a study using analytical ultracentrifugation. *Carbohydrate Research, 153*(2), 195–203. http://dx.doi.org/10.1016/S0008-6215(00)90262-3.

Li, L., Lu, Y., An, L., & Wu, C. (2013). Experimental and theoretical studies of scaling of sizes and intrinsic viscosity of hyperbranched chains in good solvents. *Journal of Chemical Physics, 138*(11), 114908. http://dx.doi.org/10.1063/1.4795577.

Listowsky, I., & Englard, S. (1968). Characterization of the far ultraviolet optically active absorption bands of sugars by circular dichrosim. *Biochemical and Biophysical Research, 30*, 329–332.

Listowsky, I., Englard, S., & Avigad, S. (1972). Conformational aspects of acidic sugars: circular dichroism studies. *Transactions of the New York Academy of Science, 34*, 218–226.

Lu, Y., An, L., & Wang, Z.-G. (2013). Intrinsic viscosity of polymers: general theory based on a partially permeable sphere model. *Macromolecules, 46*(14), 5731–5740. http://dx.doi.org/10.1021/ma400872s.

Mahendran, T., Williams, P. A., Phillips, G. O., Al-Assaf, S., & Baldwin, T. C. (2008). New insights into the structural characteristics of the Arabinogalactan–Protein AGP fraction of gum arabic. *Journal of Agricultural and Food Chemistry, 58*(1), 9269–9276.

Manrique, G. D., & Lajolo, F. M. (2002). FT-IR spectroscopy as a tool for measuring degree of methyl esterification in pectins isolated from ripening papaya fruit. *Postharvest Biology and Technology, 25*(1), 99–107. http://dx.doi.org/10.1016/S0925-5214(01)00160-0.

Mansfield, M. L., & Douglas, J. F. (2013). Shape characteristics of equilibrium and non-equilibrium fractal clusters. *Journal of Chemical Physics, 139*(4), 044901. http://dx.doi.org/10.1063/1.4813020.

Matsuhiro, B. (1996). Vibrational spectroscopy of seaweed galactans. *Hydrobiologia, 326-327*(1), 481–489.

Matsuoka, K., Yonekawa, A., Ishii, M., Honda, C., Endo, K., Moroi, Y., et al. (2006). Micellar size, shape and counterion binding of N-(1,1-Dihydroperfluoroalkyl)-N,N,N-trimethylammonium chloride in aqueous solutions. *Colloid & Polymer Science, 285*(3), 323–330. http://dx.doi.org/10.1007/s00396-006-1574-8.

Masuelli, M. A. (2013). Hydrodynamic Properties of Whole Arabic Gum. *American Journal of Food Science and Technology, 1*(3), 60–66.

Menzies, A. R., Osman, M. E., Malik, A. A., & Baldwin, T. C. (1996). A comparison of the physicochemical and immunological properties of the plant gum exudates of *Acacia senegal* (gum arabic) and *Acacia seyal* (gum tahla). *Food Additives and Contaminants, 13*(8), 991–999.

Millard, M. M., Dintzis, F. R., Willett, J. L., & Klavons, J. A. (1997). Light-scattering molecular weights and intrinsic viscosities of processed Waxy Maize starches in 90% dimethyl sulfoxide and H2O. *Cereal Chemistry, 74*(5), 687–691. http://dx.doi.org/10.1094/CCHEM.1997.74.5.687.

Moore, J. P., Farrant, J. M., & Driouich, A. (2008). A role for pectin-associated arabinans in maintaining the flexibility of the plant cell wall during water deficit stress. *Plant Signaling & Behavior, 3*(2), 102–104. http://dx.doi.org/10.1104/pp.106.077701.102.

Moore, J. P., Nguema-Ona, E., Vicré-Gibouin, M., Sørensen, I., Willats, W. G. T., Driouich, A., et al. (2013). Arabinose-rich polymers as an evolutionary strategy to plasticize resurrection plant cell walls against desiccation. *Planta, 237*(3), 739–754. http://dx.doi.org/10.1007/s00425-012-1785-9.

Nie, S.-P., Wang, C., Cui, S. W., Wang, Q., Xie, M.-Y., & Phillips, G. O. (2013a). A further amendment to the classical core structure of gum arabic (*Acacia senegal*). *Food Hydrocolloids, 31*(1), 42–48. http://dx.doi.org/10.1016/j.foodhyd.2012.09.014.

Nie, S.-P., Wang, C., Cui, S. W., Wang, Q., Xie, M.-Y., & Phillips, G. O. (2013b). The core carbohydrate structure of *Acacia seyal* var. seyal (Gum arabic). *Food Hydrocolloids, 32*(2), 221–227. http://dx.doi.org/10.1016/j.foodhyd.2012.12.027.

Pellerin, P., Doco, T., Vidal, S., Williams, P., Brillouet, J. M., & O'Neill, M. A. (1996). Structural characterization of red wine rhamnogalacturonan II. *Carbohydrate Research, 290*(2), 183–197. Retrieved from http://www.ncbi.nlm.nih.gov/pubmed/8823907.

Perris, P. J., Woessner, J. P., Waffenschmidt, S., Kilz, S., Drees, J., & Goodenough, U. W. (2001). Glycosylated polyproline II rods with kinks as a structural motif in plant hydroxyproline-rich glycoproteins. *Biochemistry, 40*, 2978–2987.

Phillips, G. O. (2009). Molecular association and function of arabinogalactan protein complexes from tree exudates. *Structural Chemistry, 20*(2), 309–315. http://dx.doi.org/10.1007/s11224-009-9422-3.

Picton, L., Bataille, I., & Muller, G. (2000). Analysis of a complex polysaccharide (gum arabic) by multi-angle laser light scattering coupled on-line to size exclusion chromatography and flow field flow fractionation. *Carbohydrate Polymers, 42*(1), 23–31.

Qi, W., Fong, C., & Lamport, D. (1991). Gum arabic glycoprotein is a twisted hairy rope. *Plant Physiology, 96*, 848–855.

Randall, R. C., Phillips, G. O., & Williams, P. A. (1989). Fractionation and characterization of gum from *Acacia senegal*. *Food Hydrocolloids, 3*(1), 65–75. Retrieved from <Go to ISI>://WOS:000207457400007.

Renard, D., Garnier, C., Lapp, A., Schmitt, C., & Sanchez, C. (2012). Structure of arabinogalactan-protein from Acacia gum: from porous ellipsoids to supramolecular architectures. *Carbohydrate Polymers, 90*(1), 322–332. http://dx.doi.org/10.1016/j.carbpol.2012.05.046.

Renard, D., Lavenant-Gourgeon, L., Ralet, M. C., & Sanchez, C. (2006). *Acacia senegal* gum: continuum of molecular species differing by their protein to sugar ratio, molecular weight, and charges. *Biomacromolecules, 7*(9), 2637–2649. http://dx.doi.org/10.1021/bm060145j.

Renard, D., Lepvrier, E., Garnier, C., Roblin, P., Nigen, M., & Sanchez, C. (2014). Structure of glycoproteins from Acacia gum: an assembly of ring-like glycoproteins modules. *Carbohydrate Polymers, 99*, 736–747. http://dx.doi.org/10.1016/j.carbpol.2013.08.090.

Roger, P., Bello-Perez, L. A., & Colonna, P. (1999). Contribution of amylose and amylopectin to the light scattering behaviour of starches in aqueous solution. *Polymer, 40*, 6897–6909. http://dx.doi.org/10.1016/S0032-3861(99)00051-8.

Rolland-Sabaté, A., Colonna, P., Mendez-Montealvo, M. G., & Planchot, V. (2007). Branching features of amylopectins and glycogen determined by asymmetrical flow field flow fractionation coupled with multiangle laser light scattering. *Biomacromolecules, 8*(8), 2520–2532. http://dx.doi.org/10.1021/bm070024z.

Rolland-Sabaté, A., Mendez-Montealvo, M. G., Colonna, P., & Planchot, V. (2008). Online determination of structural properties and observation of deviations from power law behavior. *Biomacromolecules, 9*(7), 1719–1730. http://dx.doi.org/10.1021/bm7013119.

Ross-Murphy, S. B. (1994). In S. B. Ross-Murphy (Ed.), *Physical techniques for the study of food biopolymers* (pp. 342–392). Blackie Academic & Professional.

Sanchez, C., Renard, D., Robert, P., Schmitt, C., & Lefebvre, J. (2002). Structure and rheological properties of acacia gum dispersions. *Food Hydrocolloids, 16*(3), 257–267. http://dx.doi.org/10.1016/s0268-005x(01)00096-0.

Sanchez, C., Schmitt, C., Kolodziejczyk, E., Lapp, A., Gaillard, C., & Renard, D. (2008). The acacia gum arabinogalactan fraction is a thin oblate ellipsoid: a new model based on small-angle neutron scattering and ab initio calculation. *Biophysical Journal, 94*(2), 629–639. http://dx.doi.org/10.1529/biophysj.107.109124.

Séné, C. F. B., McCann, M. C., Wilson, R. H., & Grinter, R. (1994). Fourier-transform Raman and fourier-transform Infrared spectroscopy. *Plant Physiology, 106*, 1623–1631.

Shpak, E., Barbar, E., Leykam, J. F., & Kieliszewski, M. J. (2001). Contiguous hydroxyproline residues direct hydroxyproline arabinosylation in Nicotiana tabacum. *Journal of Biological Chemistry, 276*(14), 11272–11278. http://dx.doi.org/10.1074/jbc.M011323200.

Siddig, N. E., Osman, M. E., Al-Assaf, S., Phillips, G. O., & Williams, P. A. (2005). Studies on acacia exudate gums, part IV. Distribution of molecular components in in relation to. *Food Hydrocolloids, 19*(4), 679–686. http://dx.doi.org/10.1016/j.foodhyd.2004.09.005.

Street, C. A., & Anderson, D. M. W. (1983). Refinement of structures previously proposed for gum arabic and other acacia gum exudates. *Talanta, 30*(11), 887–893.

Sweets, D., Shapiro, R., & Albershein, P. (1975). Quantitative analysis by various G.L.C. response-factor theories for partially methylated and partially ethylated alditol acetates. *Carbohydrate Research, 40*, 217–225.

Synytsya, A., Copíková, J., Matejka, P., & Machovic, V. (2003). Fourier transform Raman and infrared spectroscopy of pectins. *Carbohydrate Polymers, 54*(1), 97–106. http://dx.doi.org/10.1016/S0144-8617(03)00158-9.

Tanford, C. (1979). *Physical chemistry of macromolecules* (p. 391). John Wiley & Sons Inc.

Tao, Y., Zhang, L., Yan, F., & Wu, X. (2007). Chain conformation of water-insoluble hyperbranched polysaccharide from fungus. *Biomacromolecules, 8*(7), 2321–2328. http://dx.doi.org/10.1021/bm070335+.

Vandevelde, M., & Fenyo, J. (1985). Macromolecular distribution of *Acacia senegal* gum. *Carbohydrate Polymers, 5*(203), 251–273.

Van de Sande, W., & Persoons, A. (1985). The size and shape of macromolecular structures: determination of the radius, the length and the persistance length of rod-like micelles of dodecyldimethylammonium chloride and bromide. *Journal of Physical Chemistry, 89*(3), 404–406. http://dx.doi.org/10.1021/j100249a007.

Verbeken, D., Dierckx, S., & Dewettinck, K. (2003). Exudate gums: occurrence, production, and applications. *Applied Microbiology and Biotechnology, 63*(1), 10–21. http://dx.doi.org/10.1007/s00253-003-1354-z.

Vidal, S., Williams, P., Doco, T., Moutounet, M., & Pellerin, P. (2003). The polysaccharides of red wine: total fractionation and characterisation. *Carbohydrate Polymers, 54*, 439–447.

Vilaplana, F., & Gilbert, R. G. (2010). Characterization of branched polysaccharides using multiple-detection size separation techniques. *Journal of Separation Science, 33*(22), 3537–3554. http://dx.doi.org/10.1002/jssc.201000525.

Vinod, V. T. P., & Sashidhar, R. B. (2010). Surface morphology, chemical and structural assignment of gum Kondagogu (Cochlospermum gossypium DC.): an exudate tree gum of India. *Indian Journal of Natural Products and Resources, 1*(2), 181–192.

Wang, Q., Burchard, W., Cui, S. W., Huang, X., & Phillips, G. O. (2008). Solution properties of conventional gum arabic and a matured gum arabic (Acacia (sen) SUPER GUM). *Biomacromolecules, 9*(4), 1163–1169.

Woody, R. (1996). Theory of circular dichroism of proteins. In G. Fasman (Ed.), *Circular dichroism and the conformational analysis of biomolecules* (pp. 25–67). US: Springer. http://dx.doi.org/10.1007/978-1-4757-2508-7_2.

Yuen, S.-N., Choi, S.-M., Phillips, D. L., & Ma, C.-Y. (2009). Raman and FTIR spectroscopic study of carboxymethylated non-starch polysaccharides. *Food Chemistry, 114*(3), 1091–1098.

Young, C. Y., Missel, P. J., Mazer, N. A., Benedek, G. B., & Carey, M. C. (1978). Deduction of micellar shape from angular dissymmetry measurements of light scattered from aqueous sodium dodecyl sulfate solutions at high sodium chloride concentrations. *The Journal of Physical Chemistry, 82*(12), 1375–1378. http://dx.doi.org/10.1021/j100501a011.

Zhao, Z. D., Tan, L., Showalter, A. M., Thomas, D., Lamport, A., & Kieliszewski, M. J. (2002). Tomato LeAGP-1 arabinogalactan-protein puri ® ed from transgenic tobacco corroborates the Hyp contiguity hypothesis. *Plant Journal, 31*, 431–444.